Cosmological Structure Formation

Joel R. Primack

*Physics Department, University of California, Santa Cruz, CA 95064
USA.*

1

Cosmological Structure Formation

1.1 Introduction

Cosmology has finally become a mature science during the past decade, with predictions now routinely confirmed by observations. The modern cosmological theory is known as ΛCDM – CDM for Cold Dark Matter, particles that moved sluggishly in the early universe and thereby preserved fluctuations down to small scales (Blumenthal et al., 1984, see Fig. 1), and Λ for the cosmological constant (e.g., Lahav et al., 1991). A wide variety of large-scale astronomical observations – including the Cosmic Microwave Background (CMB), measurements of baryon acoustic oscillations (BAO), gravitational lensing, the large-scale distribution of galaxies, and the properties of galaxy clusters – agree very well with the predictions of the ΛCDM cosmology.

Like the standard model of particle physics, the ΛCDM standard cosmological model requires the determination of a number of relevant cosmological parameters, and the theory does not attempt to explain why they have the measured values – or to explain the fundamental nature of the dark matter and dark energy. These remain challenges for the future. But the good news is that the key cosmological parameters are now all determined with unprecedented accuracy, and the six-parameter ΛCDM theory provides a very good match to all the observational data including the 2015 Planck temperature and polarization data (Planck Collaboration et al., 2015a). Within uncertainties less than 1%, the Universe has critical cosmic density – i.e., $\Omega_{\text{total}} = 1.00$ and the Universe is Euclidean (or "flat") on large scales. The expansion rate of the Universe is measured by the Hubble parameter $h = 0.6774 \pm 0.0046$, and $\Omega_{\text{matter}} = 0.3089 \pm 0.0062$; this leads to the age of the Universe $t_0 = 13.799 \pm 0.021$ Gyr. The power spectrum normalization parameter is $\sigma_8 = 0.816 \pm 0.009$, and the primordial fluctuations are consistent with a purely adiabatic spectrum of fluctuations with a spec-

tral tilt $n_s = 0.968 \pm 0.006$, as predicted by single-field inflationary models (Planck Collaboration et al., 2015a). The same cosmological parameters that are such a good match to the CMB observations also predict the observed distribution of density fluctuations from small scales probed by the Lyman alpha forest[1] to the entire horizon, as shown in Fig. 2. The near-power-law galaxy-galaxy correlation function at low redshifts is now known to be a cosmic coincidence (Watson et al., 2011). I was personally particularly impressed that the evolution of the galaxy-galaxy correlations with redshift predicted by ΛCDM (Kravtsov et al., 2004) turned out to be in excellent agreement with the subsequent observations (e.g., Conroy et al., 2006).

For non-astronomers, there should be a more friendly name than ΛCDM for the standard modern cosmology. Since about 95% of the cosmic density is dark energy (either a cosmological constant with $\Omega_\Lambda = 0.69$ or some dynamical field that plays a similar cosmic role) and cold dark matter with $\Omega_{\mathrm{CDM}} = 0.26$, I recommend the simple name "Double Dark Theory" for the modern cosmological standard model (Primack and Abrams, 2006; Abrams and Primack, 2011). The contribution of ordinary baryonic matter is only $\Omega_{\mathrm{b}} = 0.05$. Only about 10% of the baryonic matter is in the form of stars or gas clouds that emit electromagnetic radiation, and the contribution of what astronomers call "metals" – chemical elements heavier than helium – to the cosmic density is only $\Omega_{\mathrm{metals}} \approx 0.0005$, most of which is in white dwarfs and neutron stars (Fukugita and Peebles, 2004). The contribution of neutrino mass to the cosmic density is $0.002 \leq \Omega_\nu \leq 0.005$, far greater than Ω_{metals}. Thus our bodies and our planet are made of the rarest form of matter in the universe: elements forged in stars and stellar explosions.

Potential challenges to ΛCDM on large scales come from the tails of the predicted distribution functions, such as CMB cold spots and massive clusters at high redshifts. However, the existing observations appear to be consistent thus far with predictions of standard ΛCDM with standard primordial power spectra; non-Gaussian initial conditions are not required (Planck Collaboration et al., 2015b). Larger surveys now underway may provide more stringent tests.

1.2 Large-Scale Structure

Large, high-resolution simulations permit detailed predictions of the distribution and properties of galaxies and clusters. From 2005-2010, the benchmark simulations were Millennium-I (Springel et al., 2005) and Millennium-

---

[1] The Lyα forest is the many absorption lines in quasar spectra due to clouds of neutral hydrogen along the line of sight to the quasar.
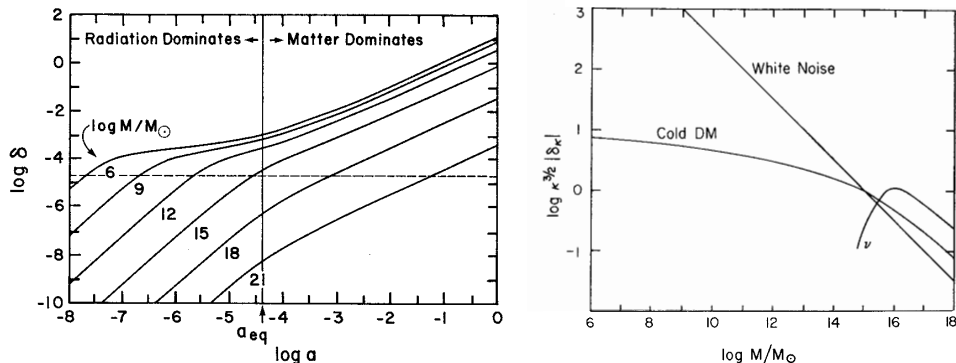
Figure 1.1 The origin of the CDM spectrum of density fluctuations. **Left panel**: Fluctuations corresponding to mass scales $10^6 M_\odot$, $10^9 M_\odot$, etc., grow proportionally to the square of scale factor a when they are outside the horizon, and when they enter the horizon (cross the horizontal dashed line) the growth of the fluctuation amplitude δ is much slower if they enter when the Universe is radiation dominated (i.e., $a < a_{\rm eq}$). Fluctuations on mass scales $> 10^{15} M_\odot$ enter the horizon after it becomes matter dominated, so their growth is proportional to scale factor a; that explains the larger separation between amplitudes for such higher-mass fluctuations. (From a 1983 conference presentation Primack and Blumenthal (1984), reprinted in Primack (1984).) **Right panel**: The resulting CDM fluctuation spectrum $(\kappa^{3/2}|\delta_\kappa| = \Delta M/M)$ is contrasted with a $\delta \propto \kappa^0$ white noise (Poisson) spectrum with the same power at all wavelengths (where wave number κ is as usual related to wavelength λ by $\kappa = 2\pi/\lambda$), and with the hot dark matter spectrum if the dark matter were light neutrinos (ν) which is cut off on galaxy mass scales by free-steaming. (From Blumenthal et al. (1984). This calculation assumed that the primordial fluctuations are scale-invariant (Zel'dovich) and that $\Omega_{\rm matter} = 1$ and Hubble parameter $h = 1$.)

II (Boylan-Kolchin et al., 2009), which have been the basis for more than 400 papers. However, these simulations used first-year Wilkinson Microwave Anisotropy Probe (WMAP) cosmological parameters, including $\sigma_8 = 0.90$, that are now in serious disagreement with the latest observations. Improved cosmological parameters, simulation codes, and computer power have permitted more accurate simulations (Kuhlen et al., 2012; Skillman et al., 2014) including Bolshoi (Klypin et al., 2011) and BigBolshoi/MultiDark (Prada et al., 2012; Riebe et al., 2013), which have recently been rerun using the Planck cosmological parameters (Klypin et al., 2014b).[2]

Dark matter halos can be characterized in a number of ways. A common one is by mass, but the mass attributed to a halo depends on a number of

---

[2] The web address for the MultiDark simulation data center is
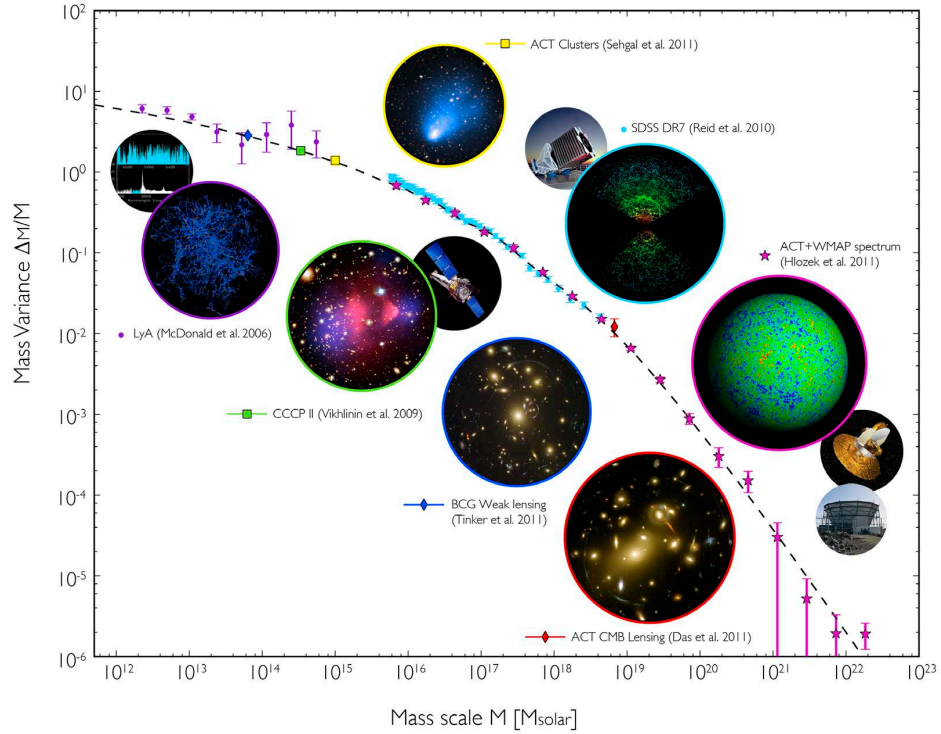http://www.cosmosim.org/cms/simulations/multidark-project/

Figure 1.2 The r.m.s. mass variance $\Delta M/M$ predicted by ΛCDM compared with observations, from CMB and the Atacama Cosmology Telescope (ACT) on large scales, brightest cluster galaxy weak lensing, clusters, the SDSS galaxy distribution, to the Lyman alpha forest on small scales. This figure highlights the consistency of power spectrum measurements by an array of cosmological probes over a large range of scales. (Redrawn from Fig. 5 in Hlozek et al. (2012), which gives the sources of the data.)

factors including how the outer edge of the halo is defined; popular choices include the spherical radius within which the average density is either 200 times critical density or the virial density (which depend on redshift). Properties of all the halos in many stored time steps of both the Bolshoi and BigBolshoi/MultiDark simulations are available on the web in the Multi-Dark database.[2] For many purposes it is more useful to characterize halos by their maximum circular velocity V_{max}, which is defined as the maximum value of $[GM(< r)/r]^{1/2}$, where G is Newton's constant and $M(< r)$ is the mass enclosed within radius r. The reason this is useful is that V_{max} is reached at a relatively low radius r_{max}, closer to the central region of a halo where stars or gas can be used to trace the velocity of the halo, while most of the halo mass is at larger radii. Moreover, the measured internal veloc-

ity of a galaxy (line of sight velocity dispersion for early-type galaxies and rotation velocity for late-type galaxies) is closely related to its luminosity according to the Faber-Jackson and Tully-Fisher relations. In addition, after a subhalo has been accreted by a larger halo, tidal stripping of its outer parts can drastically reduce the halo mass but typically decreases $V_{\max}$ much less. (Since the stellar content of a subhalo is thought to be determined before it was accreted, some authors define $V_{\max}$ to be the peak value at any redshift for the main progenitor of a halo.) Because of the observational connection between larger halo internal velocity and brighter galaxy luminosity, a common simple method of assigning galaxies to dark matter halos and subhalos is to rank order the galaxies by luminosity and the halos by $V_{\max}$, and then match them such that the number densities are comparable (Kravtsov et al., 2004; Tasitsiomi et al., 2004; Conroy et al., 2006). This is called "halo abundance matching" or (more modestly) "sub-halo abundance matching" (SHAM) (Reddick et al., 2014). Halo abundance matching using the Bolshoi simulation predicts galaxy-galaxy correlations (which are essentially counts of the numbers of pairs of galaxies at different separation distances) that are in good agreement with the Sloan Digital Sky Survey (SDSS) observations (Trujillo-Gomez et al., 2011; Reddick et al., 2013).

Abundance matching with the Bolshoi simulation also predicts galaxy velocity-mass scaling relations consistent with observations (Trujillo-Gomez et al., 2011), and a galaxy velocity function in good agreement with observations for maximum circular velocities $V_{\max} \gtrsim 100$ km/s, but higher than the HI Parkes All Sky Survey (HIPASS) and the Arecibo Legacy Fast ALFA (ALFALFA) Survey radio observations (Zwaan et al., 2010; Papastergis et al., 2011) by about a factor of 2 at 80 km/s and a factor of 10 at 50 km/s. This either means that these radio surveys are increasingly incomplete at lower velocities, or else ΛCDM is in trouble because it predicts far more small-$V_{\max}$ halos than there are observed low-V galaxies. A deeper optical survey out to 10 Mpc found no disagreement between $V_{\max}$ predictions and observations for $V_{\max} \geq 60$ km/s, and only a factor of 2 excess of halos compared to galaxies at 40 km/s (Klypin et al., 2014a). This may indicate that there is no serious inconsistency with theory, since for $V \lesssim 30$ km/s reionization and feedback can plausibly explain why there are fewer observed galaxies than dark matter halos (Bullock et al., 2000; Somerville, 2002; Benson et al., 2003; Kravtsov, 2010; Wadepuhl and Springel, 2011; Sawala et al., 2012), and also the observed scaling of metallicity with galaxy mass (Dekel and Woo, 2003; Woo et al., 2008; Kirby et al., 2011).

The radial dark matter density distribution in halos can be approximately fit by the simple formula $\rho_{\mathrm{NFW}} = 4\rho_s x^{-1}(1+x)^{-2}$, where $x \equiv r/r_s$ (Navarro

et al., 1996), and the "concentration" of a dark matter halo is defined as $C = R_{\mathrm{vir}}/R_s$ where R_{vir} is the virial radius of the halo. When we first understood that dark matter halos form with relatively low concentration $C \sim 4$ and evolve to higher concentration, we suggested that "red" galaxies that shine mostly by the light of red giant stars because they have stopped forming stars should be found in high-concentration halos while "blue" galaxies that are still forming stars should be found in younger low-concentration halos (Bullock et al., 2001). This idea was recently rediscovered by Hearin and Watson, who used the Bolshoi simulation to show that this leads to remarkably accurate predictions for the correlation functions of red and blue galaxies (Hearin and Watson, 2013; Hearin et al., 2014).

The Milky Way has two rather bright satellite galaxies, the Large and Small Magellanic Clouds. It is possible using sub-halo abundance matching with the Bolshoi simulation to determine the number of Milky-Way-mass dark matter halos that have subhalos with high enough circular velocity to host such satellites. It turns out that about 55% have no such subhalos, about 28% have one, about 11% have two, and so on (Busha et al., 2011a). Remarkably, these predictions are in excellent agreement with an analysis of observations by the Sloan Digital Sky Survey (SDSS) (Liu et al., 2011). The distribution of the relative velocities of central and bright satellite galaxies from SDSS spectroscopic observations is also in very good agreement with the predictions of the Millennium-II simulation (Tollerud et al., 2011), and the Milky Way's lower-luminosity satellite population is not unusual (Strigari and Wechsler, 2012). Considered in a cosmological context, the Magellanic clouds are likely to have been accreted within about the last Gyr (Besla et al., 2012), and the Milky Way halo mass is $1.2^{+0.7}_{-0.4}(\mathrm{stat.})\pm0.3(\mathrm{sys.})\times10^{12}M_\odot$ (Busha et al., 2011b).

1.3 Galaxy Formation

At early times, for example the CMB epoch about 400,000 years after the big bang, or on very large scales at later times, linear calculations starting from the ΛCDM fluctuation spectrum allow accurate predictions. But on scales where structure forms, the fluctuations have grown large enough that they are strongly nonlinear, and we must resort to simulations. The basic idea is that regions that start out with slightly higher than average density expand a little more slowly than average because of gravity, and regions that start out with slightly lower density expand a little faster. Nonlinear structure forms by the process known by the somewhat misleading name "gravitational collapse" – misleading because what really happens is that when positive
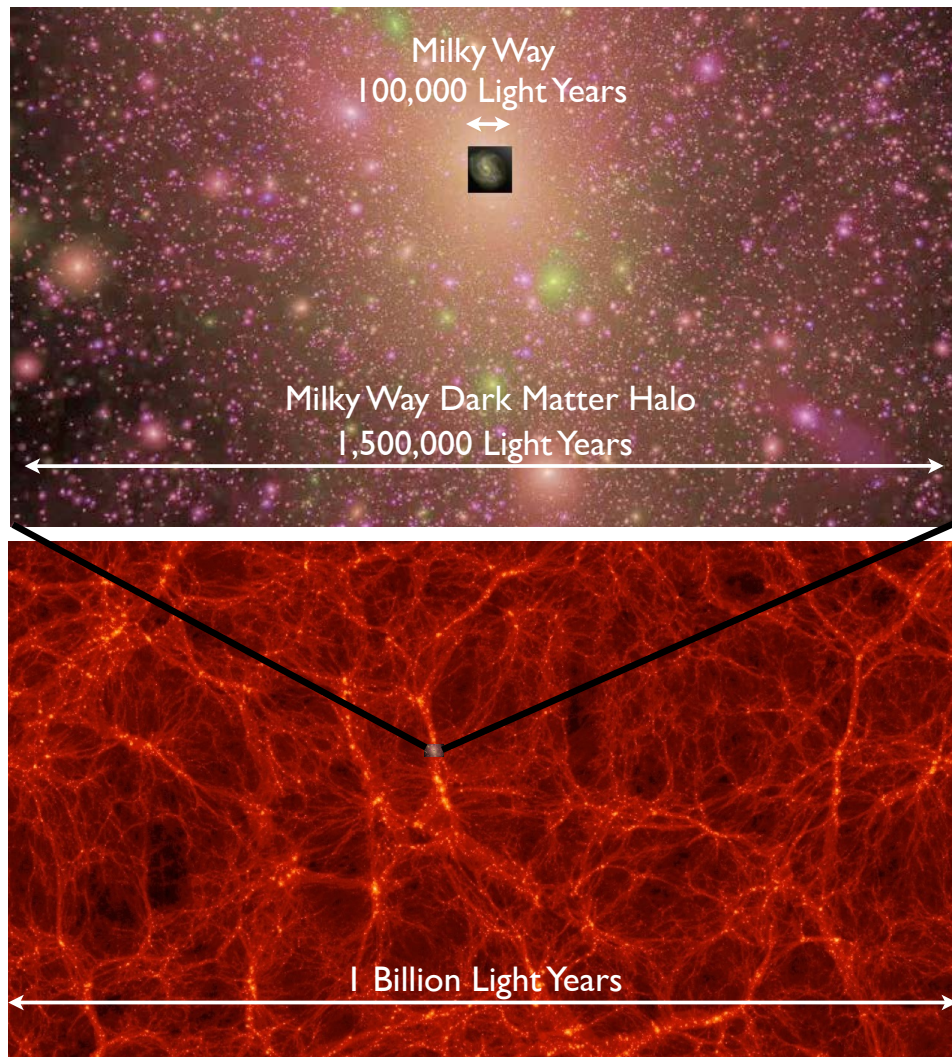
Figure 1.3 The stellar disk of a large spiral galaxy like the Milky Way is about 100,000 light years across, which is tiny compared with the dark matter halo of such a galaxy (from the Aquarius dark matter simulation Springel et al., 2008), and even much smaller compared with the large-scale cosmic web (from the Bolshoi simulation Klypin et al., 2011).

fluctuations have grown sufficiently that they are about twice as dense as typical regions their size, they stop expanding while the surrounding universe keeps expanding around them. The result is that regions that collapse earlier are denser than those that collapse later; thus galaxy dark matter halos are denser than cluster halos. The visible galaxies form because the ordinary

baryonic matter can radiate away its kinetic energy and fall toward the centers of the dark matter halos; when the ordinary matter becomes dense enough it forms stars. Thus visible galaxies are much smaller than their host dark matter halos, which in turn are much smaller than the large scale structure of the cosmic web, as shown in Fig. 3.

Astronomical observations represent snapshots of moments long ago when the light we now observe left distant astronomical objects. It is the role of astrophysical theory to produce movies – both metaphorical and actual – that link these snapshots together into a coherent physical picture. To predict cosmological large-scale structures, it has been sufficient to treat all the mass as dark matter in order to calculate the growth of structure and dark matter halo properties. But hydrodynamic simulations – i.e., including baryonic matter – are necessary to treat the formation and evolution of galaxies.
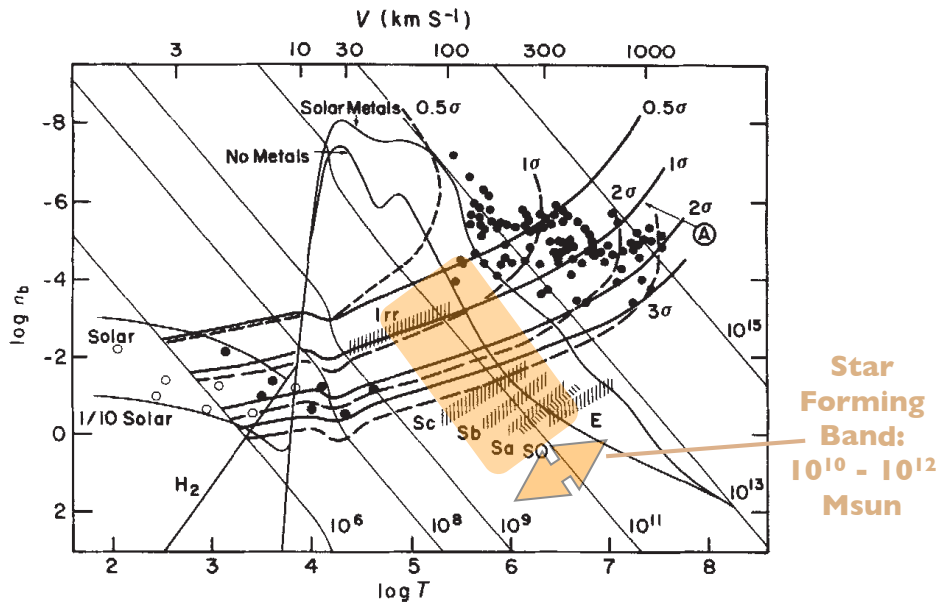

Figure 1.4 The Star-Forming Band on a diagram of baryon density n_b versus the three-dimensional r.m.s. velocity dispersion V and virial temperature T for structures of various sizes in the universe, where $T = \mu V^2/3k$, μ is mean molecular weight (≈ 0.6 for ionized primordial H + He) and k is Boltzmann's constant. Below the No Metals and Solar Metals cooling curves, the cooling timescale is more rapid than the gravitational timescale. Dots are groups and clusters. Diagonal lines show the halo masses in units of $M_\odot$. (This is Fig. 3 in Blumenthal et al., 1984, with the Star-Forming Band added.)

An old criticism of ΛCDM has been that the order of cosmogony is wrong: halos grow from small to large by accretion in a hierarchical formation theory like ΛCDM, but the oldest stellar populations are found in the most massive galaxies – suggesting that these massive galaxies form earliest, a phenomenon known as "downsizing" (Cowie et al., 1996). The key to explaining the downsizing phenomenon is the realization that star formation is most efficient in dark matter halos with masses in the band between about 10^{10} and $10^{12} M_\odot$ (Fig. 1 bottom in Behroozi et al., 2013). This goes back at least as far as the original Cold Dark Matter paper (Blumenthal et al., 1984): see Fig. 4. A dark matter halo that has the total mass of a cluster of galaxies today will have crossed this star-forming mass band at an early epoch, and it will therefore contain galaxies whose stars formed early. These galaxies will be red and dead today. A less massive dark matter halo that is now entering the star-forming band today will just be forming significant numbers of stars, and it will be blue today. The details of the origin of the star-forming band are still being worked out. Back in 1984, we argued that cooling would be inefficient for masses greater than about $10^{12} M_\odot$ because the density would be too low, and inefficient for masses less than about $10^8 M_\odot$ because the gas would not be heated enough by falling into these small potential wells. Now we know that reionization, supernovae (Dekel and Silk, 1986), and other energy input additionally impedes star formation for halo masses below about $10^{10} M_\odot$, and feedback from active galactic nuclei (AGN) additionally impedes star formation for halo masses above about $10^{12} M_\odot$.

Early simulations of disk galaxy formation found that the stellar disks had much lower rotation velocities than observed galaxies (Navarro and Steinmetz, 2000). This problem seemed so serious that it became known as the "angular momentum catastrophe." A major cause of this was excessive cooling of the gas in small halos before they merged to form larger galaxies (Maller and Dekel, 2002). Simulations with better resolution and more physical treatment of feedback from star formation appear to resolve this problem. In particular, the Eris cosmological simulation (Guedes et al., 2011) produced a very realistic spiral galaxy, as have many simulations since then. Somerville and Davé (2014) is an excellent recent review of progress in understanding galaxy formation. In the following I summarize some of the latest developments. There are now two leading approaches to simulating galaxies:

- Low resolution, ~ 1 kiloparsecs. The **advantages** of this approach are that it is possible to simulate many galaxies and study galaxy popula-

tions and their interactions with the circumgalactic and intergalactic media, but the **disadvantages** are that we learn relatively little about how galaxies themselves form and evolve at high redshifts. The prime examples of this approach now are the *Illustris* (Vogelsberger et al., 2014b) and EAGLE (Schaye et al., 2015) simulations. Like semi-analytic models of galaxy formation (reviewed in Benson, 2010), these projects adjusted the parameters governing star-formation and feedback processes in order to reproduce key properties of galaxies at the present epoch, redshift $z = 0$. The *Illustris* simulation in a volume $(106.5\mathrm{Mpc})^3$ forms $\sim 40,000$ galaxies at the present epoch with a reasonable mix of elliptical and spiral galaxies that have realistic appearances (Snyder et al., 2015), obey observed scaling relations, have the observed numbers of galaxies as a function of their luminosity, and were formed with the observed cosmic star formation rate (Vogelsberger et al., 2014a). It forms massive compact galaxies by redshift $z = 2$ via central starbursts in major mergers of gas-rich galaxies or else by assembly at very early times (Wellons et al., 2015). Remarkably, the *Illustris* simulation also predicts a population of damped Lyman α absorbers (DLAs, small-galaxy-size clouds of neutral hydrogen) that agrees with some of the key observational properties of DLAs (Bird et al., 2014, 2015). The EAGLE simulation in volumes up to $(100\mathrm{Mpc})^3$ reproduces the observed galaxy mass function from 10^8 to $10^{11} M_\odot$ at a level of agreement close to that attained by semi-analytic models (Schaye et al., 2015), and the observed atomic and molecular hydrogen content of galaxies out to $z \sim 3$ (Rahmati et al., 2015; Lagos et al., 2015).

- High resolution, ~ 10s of parsecs. The **advantages** are that it is possible to compare simulation outputs in detail with high-redshift galaxy images and spectra to discover the drivers of morphological changes as galaxies evolve, but the **disadvantage** is that such simulations are so expensive computationally that it is as yet impossible to run enough cases to create statistical samples. Leading examples of this approach are FIRE simulations led by Phil Hopkins (e.g., Hopkins et al., 2014) and the ART simulation suite led by Avishai Dekel and myself (e.g., Zolotov et al., 2014). We try to compensate for the small number of high-resolution simulations by using simulation outputs to tune semi-analytic models, which in turn use cosmological dark-matter-only simulations like Bolshoi to follow the evolution of $\sim 10^6$ galaxies in their cosmological context (e.g., Porter et al., 2014b,a; Brennan et al., 2015).

The high-resolution FIRE simulations, based on the GIZMO smooth particle hydrodynamics code (Hopkins, 2014) with supernova and stellar feed-

back, including radiative feedback (RF) pressure from massive stars, treated with zero adjusted parameters, reproduce the observed relation between stellar and halo mass up to $M_{\mathrm{halo}} \sim 10^{12} M_{\odot}$ and the observed star formation rates Hopkins et al. (2014). FIRE simulations predict covering fractions of neutral hydrogen with column densities from $10^{17} \mathrm{cm}^{-2}$ (Lyman limit systems, LLS) to $> 10^{20.3} \mathrm{cm}^{-2}$ (DLAs) in agreement with observations at redshifts z=2-2.5 (Faucher-Giguère et al., 2015); this success is a consequence of the simulated galactic winds. FIRE simulations also correctly predict the observed evolution of the decrease of metallicity with stellar mass (Ma et al., 2015), and produce dwarf galaxies that appear to agree with observations (Oñorbe et al., 2015) as we will discuss in more detail below.

The high-resolution simulation suite based on the ART adaptive mesh refinement (AMR) approach (Kravtsov et al., 1997; Ceverino and Klypin, 2009) incorporates at the sub-grid level many of the physical processes relevant for galaxy formation. Our initial group of 30 zoom-in simulations of galaxies in dark matter halos of mass $(1 - 30) \times 10^{12} M_{\odot}$ at redshift $z = 1$ were run at 35-70 pc maximum (physical) resolution (Ceverino et al., 2012, 2015a). The second group of 35 simulations (VELA01 to VELA35) with 17.5 to 35 pc resolution of halos of mass $(2 - 20) \times 10^{11} M_{\odot}$ at redshift $z = 1$have now been run three times with varying inclusion of radiative pressure feedback (none, UV, UV+IR), as described in Ceverino et al. (2014). RF pressure including the effects of stellar winds (Hopkins et al., 2012, 2014) captures essential features of star formation in our simulations. In particular, RF begins to affect the star-forming region as soon as massive stars form, long before the first supernovae occur, and the amount of energy released in RF greatly exceeds that released by supernovae (Ceverino et al., 2014; Trujillo-Gomez et al., 2015). In addition to radiation pressure, the local UV flux from young star clusters also affects the cooling and heating processes in star-forming regions through photoheating and photoionization. We use our *Sunrise* code (Jonsson, 2006; Jonsson et al., 2006, 2010; Jonsson and Primack, 2010) to make realistic images and spectra of these simulated galaxies in many wavebands and at many times during their evolution, including the effects of stellar evolution and of dust scattering, absorption, and re-emission, to compare with the imaging and photometry from CANDELS[3] and other surveys – see Fig. 5 for examples including the effect of CANDELization (reducing the resolution and adding noise) to allow direct comparison with HST images.

In comparing our simulations with HST observations, especially those from the CANDELS and 3D-HST surveys, we are finding that the simula-

---

[3] CANDELS, the Cosmic Assembly Near-infrared Deep Extragalactic Legacy Survey, was the largest-ever Hubble Space Telescope survey, see `http://candels.ucolick.org/`.
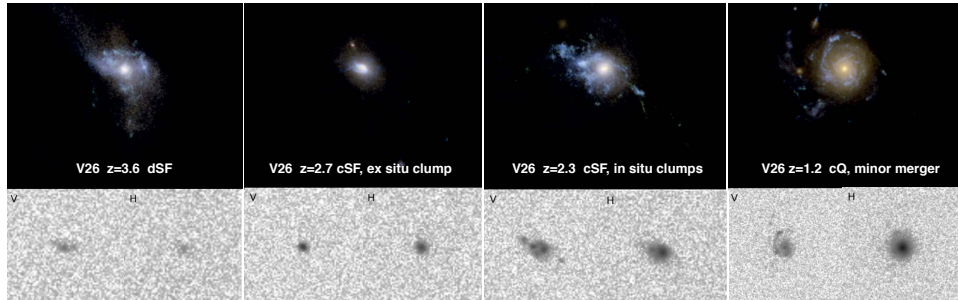
Figure 1.5 Face-on images of Vela26 simulated galaxy with UV radiation pressure feedback, at four redshifts **(a)** $z = 3.6$ when it is diffuse and star forming (dSF); **(b)** $z = 2.7$ when it has become compact and star forming (cSF) with a red ex-situ clump; **(c)** $z = 2.3$ still cSF, now with in situ clumps apparent in the V-band image; **(d)** compact and quenched (cQ) during a minor merger, with tidal features visible in the V-band image. Top panels: three-color composite images at high resolution; bottom panels: CANDELized V and H band images. The observed V band images correspond to ultraviolet radiation from massive young stars in the galaxy rest frame, while the observed H band images show optical light from the entire stellar population including old stars. The CANDELS survey took advantage of the infrared capability of the Wide Field Camera 3, installed on the last service visit to HST in 2009.

tions can help us interpret a variety of observed phenomena that we now realize are important in galaxy evolution. One is the **formation of compact galaxies**. Analysis of CANDELS images suggested (Barro et al., 2013, 2014a,b) that diffuse star-forming galaxies become compact galaxies (blue nuggets) which subsequently quench (red nuggets). We see very similar behavior in our VELA simulations with UV radiative feedback (Zolotov et al., 2014, see Figure 2), and we have identified in our simulations several mechanisms that lead to compaction often followed by rapid quenching, including major gas-rich mergers, disk instabilities often triggered by minor mergers, and opposing gas flows into the central galaxy (Danovich et al., 2015).

Another aspect of galaxy formation seen in HST observations is **massive star-forming clumps** (Guo et al., 2012; Wuyts et al., 2013, and references therein), which occur in a large fraction of star-forming galaxies at redshifts z = 1-3 (Guo et al., 2015). In our simulations there are two types of clumps. Some are a stage of minor mergers – we call those ex situ clumps. A majority of the clumps originate in situ from violent disk instabilities (VDI) in gas-rich galaxies (Ceverino et al., 2012; Moody et al., 2014; Mandelker et al., 2014). Some of these in situ clumps are associated with gas instabilities that help to create compact spheroids, and some form after the central spheroid

and are associated with the formation of surrounding disks. We find that there is not a clear separation between these processes, since minor mergers often trigger disk instabilities in our simulations (Zolotov et al., 2014).

Star-forming galaxies with stellar masses $M_* \lesssim 3 \times 10^9 M_\odot$ at $z > 1$ have recently been shown to have mostly **elongated (prolate) stellar distributions** (van der Wel et al., 2014) rather than disks or spheroids, based on their observed axis ratio distribution. In our simulations this occurs because most dark matter halos are prolate especially at small radii (Allgood et al., 2006), and the first stars form in these elongated inner halos; at lower redshifts, as the stars begin to dominate the dark matter, the galaxy centers become disky or spheroidal (Ceverino et al., 2015b).

Both the FIRE and ART simulation groups and many others are participating in the Assembling Galaxies of Resolved Anatomy (AGORA) collaboration (Kim et al., 2014) to run high-resolution simulations of the same initial conditions with halos of masses 10^{10}, 10^{11}, 10^{12}, and $10^{13} M_\odot$ at $z = 0$ with as much as possible the same astrophysical assumptions. AGORA cosmological runs using different simulation codes will be systematically compared with each other using a common analysis toolkit and validated against observations to verify that the solutions are robust – i.e., that the astrophysical assumptions are responsible for any success, rather than artifacts of particular implementations. The goals of the AGORA project are, broadly speaking, to raise the realism and predictive power of galaxy simulations and the understanding of the feedback processes that regulate galaxy "metabolism."

It still remains to be seen whether the entire population of galaxies can be explained in the context of ΛCDM. A concern regarding disk galaxies is whether the formation of bulges by both galaxy mergers and secular evolution will prevent the formation of as many pure disk galaxies as we see in the nearby universe (Kormendy and Fisher, 2008). A concern regarding massive galaxies is whether theory can naturally account for the relatively large number of ultra-luminous infrared galaxies. The bright sub-millimeter galaxies were the greatest discrepancy between our semi-analytic model predictions compared with observations out to high redshift (Somerville et al., 2012). This could possibly be explained by a top-heavy stellar initial mass function, or perhaps more plausibly by more realistic simulations including self-consistent treatment of dust (Hayward et al., 2011, 2013). Clearly, there is much still to be done, both observationally and theoretically. It is possible that all the potential discrepancies between ΛCDM and observations of relatively massive galaxies will be resolved by better understanding of the complex astrophysics of their formation and evolution. But small galaxies might provide more stringent tests of ΛCDM.

1.4 Smaller Scale Issues: Cusps

Cusps were perhaps the first potential discrepancy pointed out between the dark matter halos predicted by CDM and the observations of small galaxies that appeared to be dominated by dark matter nearly to their centers (Flores and Primack, 1994; Moore, 1994). Pure dark matter simulations predicted that the central density of dark matter halos behaves roughly as $\rho \sim r^{-1}$. As mentioned above, dark matter halos have a density distribution that can be roughly approximated as $\rho_{\mathrm{NFW}} = 4\rho_s x^{-1}(1+x)^{-2}$, where $x \equiv r/r_s$ (Navarro et al., 1996). But this predicted r^{-1} central cusp in the dark matter distribution seemed inconsistent with published observations of the rotation velocity of neutral hydrogen as a function of radius.

In small galaxies with significant stellar populations, simulations show that central starbursts can naturally produce relatively flat density profiles (Governato et al., 2010, 2012; Pontzen and Governato, 2012; Teyssier et al., 2013; Brooks, 2014; Brooks and Zolotov, 2014; Madau et al., 2014; Oñorbe et al., 2015; Nipoti and Binney, 2015). Gas cools into the galaxy center and becomes gravitationally dominant, adiabatically pulling in some of the dark matter (Blumenthal et al., 1986; Gnedin et al., 2011). But then the gas is driven out very rapidly by supernovae and the entire central region expands, with the density correspondingly dropping. Several such episodes can occur, producing a more or less constant central density consistent with observations, as shown in Fig. 6. The figure shows that galaxies in the THINGS sample are consistent with ΛCDM hydrodynamic simulations. But simulated galaxies with stellar mass less than about $3 \times 10^6 M_\odot$ may have cusps, although Oñorbe et al. (2015) found that stellar effects can soften the cusp in even lower-mass galaxies if the star formation is extended in time. The observational situation is unclear. In Sculptor and Fornax, the brightest dwarf spheroidal satellite galaxies of the Milky Way, stellar motions may imply a flatter central dark matter radial profile than $\rho \sim r^{-1}$ (Walker and Peñarrubia, 2011; Amorisco and Evans, 2012; Jardel and Gebhardt, 2012). However, other papers have questioned this (Jardel and Gebhardt, 2013; Breddels and Helmi, 2013, 2014; Richardson and Fairbairn, 2014).

Will baryonic effects explain the radial density distributions in larger low surface brightness (LSB) galaxies? These are among the most common galaxies. They have a range of masses but many have fairly large rotation velocities indicating fairly deep potential wells, and many of them may not have enough stars for the scenario just described to explain the observed rotation curves (Kuzio de Naray and Spekkens, 2011). Can we understand the observed distribution of the $\Delta_{1/2}$ measure of central density (Alam et al.,
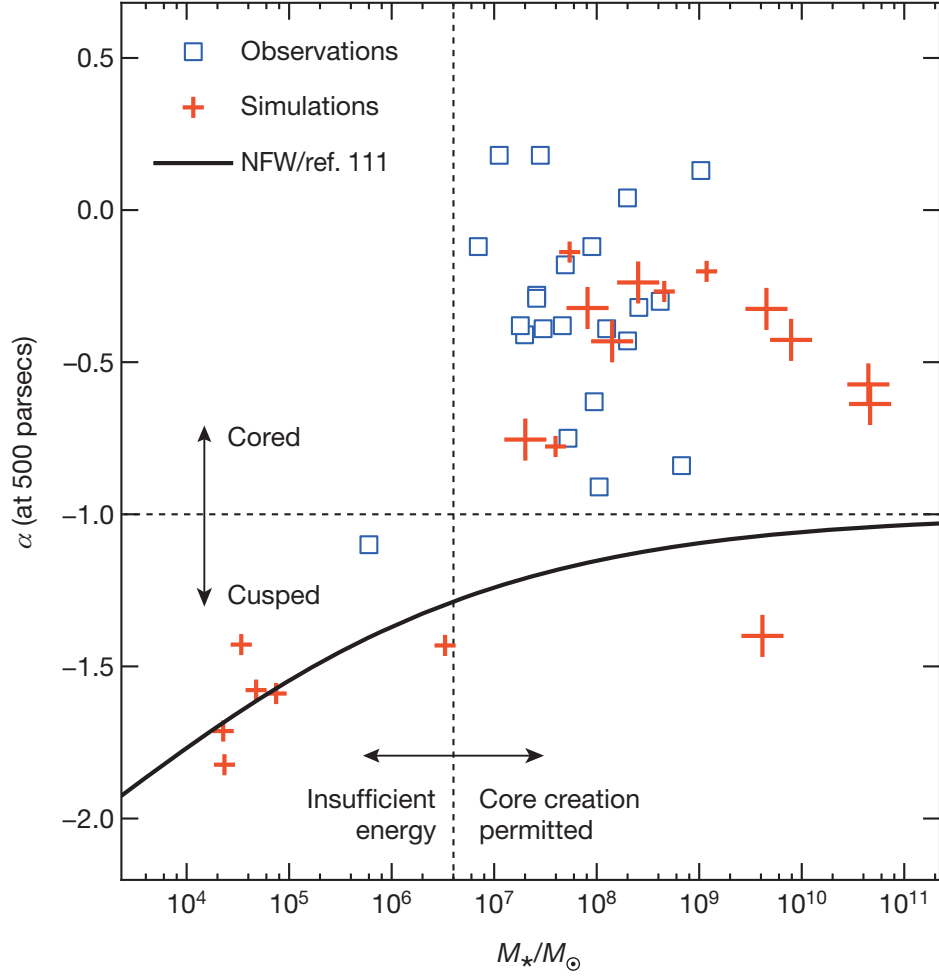
Figure 1.6 Dark matter cores are generated by baryonic effects in galaxies with sufficient stellar mass. The slope α of the dark matter central density profile r^α is plotted vs. stellar mass measured at 500 parsecs from simulations described in Pontzen and Governato (2012). The solid NFW curve assumes the halo concentrations given by (Macciò et al., 2007). Large crosses: halos with $> 5 \times 10^5$ dark matter particles; small crosses: $> 5 \times 10^4$ particles. Squares represent galaxies observed by The HI Nearby Galaxy Survey (THINGS). (Fig. 3 in Pontzen and Governato 2014.)

2002) and the observed diversity of rotation curves (Macciò et al., 2012b; Oman et al., 2015)? This is a challenge for galaxy simulators.

Some authors have proposed that warm dark matter (WDM), with initial velocities large enough to prevent formation of small dark matter halos,

could solve some of these problems. However, that does not appear to work: the systematics of galactic radial density profiles predicted by WDM do not at all match the observed ones (Kuzio de Naray et al., 2010; Macciò et al., 2012a, 2013). WDM that's warm enough to affect galaxy centers may not permit early enough galaxy formation to reionize the universe (Governato et al., 2015). Yet another constraint on WDM is the evidence for a great deal of dark matter substructure in galaxy halos (Zentner and Bullock, 2003), discussed further below.

1.5 Smaller Scale Issues: Satellite Galaxies

As the top panel of Fig. 3 shows, ΛCDM predicts that there are many fairly massive subhalos within dark matter halos of galaxies like the Milky Way and the Andromeda galaxy, more than there are observed satellite galaxies (Klypin et al., 1999; Moore et al., 1999). This is not obviously a problem for the theory since reionization, stellar feedback, and other phenomena are likely to suppress gas content and star formation in low-mass satellites. As more faint satellite galaxies have been discovered, especially using multicolor information from SDSS observations, the discrepancy between the predicted and observed satellite population has been alleviated. Many additional satellite galaxies are predicted to be discovered by deeper surveys (e.g., Bullock et al., 2010), including those in the Southern Hemisphere seen by the Dark Energy Survey (The DES Collaboration et al., 2015) and eventually the Large Synoptic Survey Telescope (LSST).

However, a potential discrepancy between theory and observations is the "too big to fail" (TBTF) problem (Boylan-Kolchin et al., 2011, 2012). The Via Lactea-II high-resolution dark-matter-only simulation of a Milky Way size halo (Diemand et al., 2007, 2008) and the six similar Aquarius simulations (Springel et al., 2008) all have several subhalos that are too dense in their centers to host any observed Milky Way satellite galaxy. The brightest observed dwarf spheroidal (dSph)satellites all have $12 \lesssim V_{\max} \lesssim 25$ km/s. But the Aquarius simulations predict at least 10 subhalos with $V_{\max} > 25$ km/s. These halos are also among the most massive at early times, and thus are not expected to have had their star formation greatly suppressed by reionization. They thus appear to be too big to fail to become observable satellites (Boylan-Kolchin et al., 2012).

The TBTF problem is closely related to the cusp-core issue, since TBTF is alleviated by any process that lowers the central density and thus the internal velocity of satellite galaxies. Many of the papers finding that baryonic effects remove central cusps cited in the previous section are thus also arguments

against TBTF. A recent simulation of regions like the Local Group found the number, internal velocities, and distribution of the satellite galaxies to be very comparable with observations (Sawala et al., 2014).

Perhaps there is additional physics beyond ΛCDM that comes into play on small scales. One possibility that has been investigated is warm dark matter (WDM). A simulation like Aquarius but with WDM has fewer high-$V_{\max}$ halos (Lovell et al., 2012). But it is not clear that such WDM simulations with the lowest WDM particle mass allowed by the Lyman alpha forest and other observations (Viel et al., 2013; Horiuchi et al., 2014) will have enough substructure to account for the observed faint satellite galaxies (e.g., Polisensky and Ricotti, 2011), and as already mentioned WDM does not appear to be consistent with observed systematics of small galaxies.

Another possibility is that the dark matter particles interact with themselves much more strongly than they interact with ordinary matter (Spergel and Steinhardt, 2000). There are strong constraints on such self-interacting dark matter (SIDM) from colliding galaxy clusters (Harvey et al., 2015; Massey et al., 2015), and in hydrodynamic simulations of dwarf galaxies SIDM has similar central cusps to CDM (Bastidas Fry et al., 2015). SIDM can be velocity-dependent, at the cost of adding additional parameters, and if the self-interaction grows with an inverse power of velocity the effects can be strong in dwarf galaxies (Elbert et al., 2014). An Aquarius-type simulation but with velocity-dependent SIDM produced subhalos with inner density structure that may be compatible with the bright dSph satellites of the Milky Way (Vogelsberger et al., 2012). Whether higher-resolution simulations of this type will turn out to be consistent with observations remains to be seen.

1.6 Smaller Scale Issues: Dark Matter Halo Substructure

The first strong indication of galaxy dark matter halo substructure was the flux ratio anomalies seen in quadruply imaged radio quasars ("radio quads") (Metcalf and Madau, 2001; Dalal and Kochanek, 2002; Metcalf and Zhao, 2002). Smooth mass models of lensing galaxies can easily explain the observed positions of the images, but the predictions of such models of the corresponding fluxes are frequently observed to be strongly violated. Optical and X-ray quasars have such small angular sizes that the observed optical and X-ray flux anomalies can be caused by stars ("microlensing"), which has allowed a measurement of the stellar mass along the lines of sight in lensing galaxies (Pooley et al., 2012). But because the quasar radio-emitting region is larger, the observed radio flux anomalies can only be caused by

relatively massive objects, with masses of order 10^6 to $10^8 M_\odot$ along the line of sight. After some controversy regarding whether ΛCDM simulations predict enough dark matter substructure to account for the observations, the latest papers concur that the observations are consistent with standard theory, taking into account uncertainty in lens system ellipticity (Metcalf and Amara, 2012) and intervening objects along the line of sight (Xu et al., 2012, 2015). But this analysis is based on a relatively small number of observed systems (Table 2 of Chen et al. (2011) lists the 10 quads that have been observed in the radio or mid-IR), and further observational and theoretical work would be very helpful.

Another gravitational lensing indication of dark matter halo substructure consistent with ΛCDM simulations comes from detailed analysis of galaxy-galaxy lensing (Vegetti et al., 2010, 2012, 2014), although much more such data will need to be analyzed to get strong constraints. Other gravitational lensing observations including time delays can probe the structure of dark matter halos in new ways (Keeton and Moustakas, 2009). Hezaveh et al. (2013, 2014) show that dark matter substructure can be detected using spatially resolved spectroscopy of gravitationally lensed dusty galaxies observed with ALMA. Nierenberg et al. (2014) demonstrates that subhalos can be detected using strongly lensed narrow-line quasar emission, as originally proposed by Moustakas and Metcalf (2003).

The great thing about gravitational lensing is that it directly measures mass along the line of sight. This can provide important information that is difficult to obtain in other ways. For example, the absence of anomalous skewness in the distribution of high redshift Type 1a supernovae brightnesses compared with low redshift ones implies that massive compact halo objects (MACHOs) in the enormous mass range 10^{-2} to $10^{10} M_\odot$ cannot be the main constituent of dark matter in the universe (Metcalf and Silk, 2007). The low observed rate of gravitational microlensing of stars in the Large and Small Magellanic clouds by foreground compact objects implies that MACHOs in the mass range between 0.6×10^{-7} and $15 M_\odot$ cannot be a significant fraction of the dark matter in the halo of the Milky Way (Tisserand et al., 2007). Gravitational microlensing could even detect free-floating planets down to $10^{-8} M_\odot$, just one percent of the mass of the earth (Strigari et al., 2012).

A completely independent way of determining the amount of dark matter halo substructure is to look carefully at the structure of dynamically cold stellar streams. Such streams come from the tidal disruption of small satellite galaxies or globular clusters. In numerical simulations, the streams suffer many tens of impacts from encounters with dark matter substructures of mass 10^5 to $10^7 M_\odot$ during their lifetimes, which create fluctuations

in the stream surface density on scales of a few degrees or less. The observed streams contain just such fluctuations (Yoon et al., 2011; Carlberg, 2012; Carlberg et al., 2012; Carlberg and Grillmair, 2013), so they provide strong evidence that the predicted population of subhalos is present in the halos of galaxies like the Milky Way and M31. Comparing additional observations of dynamically cold stellar streams with fully self-consistent simulations will give more detailed information about the substructure population. The Gaia spacecraft's measurements of the positions and motions of vast numbers of Milky Way stars will be helpful in quantifying the nature of dark matter substructure (Ngan and Carlberg, 2014; Feldmann and Spolyar, 2015).

1.7 Conclusions

ΛCDM appears to be extremely successful in predicting the cosmic microwave background and large-scale structure, including the observed distribution of galaxies both nearby and at high redshift. It has therefore become the standard cosmological framework within which to understand cosmological structure formation, and it continues to teach us about galaxy formation and evolution. For example, I used to think that galaxies are pretty smooth, that they generally grow in size as they evolve, and that they are a combination of disks and spheroids. But as I discussed in Section 3, HST observations combined with high-resolution hydrodynamic simulations are showing that most star-forming galaxies are very clumpy; that galaxies often undergo compaction, which reduces their radius and greatly increases their central density; and that most lower-mass galaxies are not spheroids or disks but are instead elongated when their centers are dominated by dark matter.

ΛCDM faces challenges on smaller scales. Although starbursts can rapidly drive gas out of the central regions of galaxies and thereby reduce the central dark matter density, it remains to be seen whether this and/or other baryonic physics can explain the observed rotation curves of the entire population of dwarf and low surface brightness (LSB) galaxies. If not, perhaps more complicated physics such as self-interacting dark matter may be needed. But standard ΛCDM appears to be successful in predicting the dark matter halo substructure that is now observed via gravitational lensing and stellar streams, and any alternative theory must do at least as well.

References

Abrams, Nancy Ellen, and Primack, Joel R. 2011. *The New Universe and the Human Future: How a Shared Cosmology Could Transform the World.* Yale University Press.

Alam, S. M. K., Bullock, J. S., and Weinberg, D. H. 2002. Dark Matter Properties and Halo Central Densities. *ApJ*, **572**(June), 34–40.

Allgood, B., Flores, R. A., Primack, J. R., Kravtsov, A. V., Wechsler, R. H., Faltenbacher, A., and Bullock, J. S. 2006. The shape of dark matter haloes: dependence on mass, redshift, radius and formation. *MNRAS*, **367**(Apr.), 1781–1796.

Amorisco, N. C., and Evans, N. W. 2012. Dark matter cores and cusps: the case of multiple stellar populations in dwarf spheroidals. *MNRAS*, **419**(Jan.), 184–196.

Barro, G., Faber, S. M., Pérez-González, P. G., Koo, D. C., Williams, C. C., Kocevski, D. D., Trump, J. R., Mozena, M., McGrath, E., van der Wel, A., Wuyts, S., Bell, E. F., Croton, D. J., Ceverino, D., Dekel, A., Ashby, M. L. N., Cheung, E., Ferguson, H. C., Fontana, A., Fang, J., Giavalisco, M., Grogin, N. A., Guo, Y., Hathi, N. P., Hopkins, P. F., Huang, K.-H., Koekemoer, A. M., Kartaltepe, J. S., Lee, K.-S., Newman, J. A., Porter, L. A., Primack, J. R., Ryan, R. E., Rosario, D., Somerville, R. S., Salvato, M., and Hsu, L.-T. 2013. CANDELS: The Progenitors of Compact Quiescent Galaxies at $z \sim 2$. *ApJ*, **765**(Mar.), 104.

Barro, G., Faber, S. M., Pérez-González, P. G., Pacifici, C., Trump, J. R., Koo, D. C., Wuyts, S., Guo, Y., Bell, E., Dekel, A., Porter, L., Primack, J., Ferguson, H., Ashby, M. L. N., Caputi, K., Ceverino, D., Croton, D., Fazio, G. G., Giavalisco, M., Hsu, L., Kocevski, D., Koekemoer, A., Kurczynski, P., Kollipara, P., Lee, J., McIntosh, D. H., McGrath, E., Moody, C., Somerville, R., Papovich, C., Salvato, M., Santini, P., Tal, T., van der Wel, A., Williams, C. C., Willner, S. P., and Zolotov, A. 2014a. CANDELS+3D-HST: Compact SFGs at $z \sim 2 - 3$, the Progenitors of the First Quiescent Galaxies. *ApJ*, **791**(Aug.), 52.

Barro, G., Trump, J. R., Koo, D. C., Dekel, A., Kassin, S. A., Kocevski, D. D., Faber, S. M., van der Wel, A., Guo, Y., Pérez-González, P. G., Toloba, E., Fang, J. J., Pacifici, C., Simons, R., Campbell, R. D., Ceverino, D., Finkelstein, S. L., Goodrich, B., Kassis, M., Koekemoer, A. M., Konidaris, N. P., Livermore, R. C., Lyke, J. E., Mobasher, B., Nayyeri, H., Peth, M., Primack,

J. R., Rizzi, L., Somerville, R. S., Wirth, G. D., and Zolotov, A. 2014b. Keck-I MOSFIRE Spectroscopy of Compact Star-forming Galaxies at $z \gtrsim 2$: High Velocity Dispersions in Progenitors of Compact Quiescent Galaxies. *ApJ*, **795**(Nov.), 145.

Bastidas Fry, A., Governato, F., Pontzen, A., Quinn, T., Tremmel, M., Anderson, L., Menon, H., Brooks, A. M., and Wadsley, J. 2015. All about baryons: revisiting SIDM predictions at small halo masses. *ArXiv e-prints*, Jan.

Behroozi, P. S., Wechsler, R. H., and Conroy, C. 2013. On the Lack of Evolution in Galaxy Star Formation Efficiency. *ApJL*, **762**(Jan.), L31.

Benson, A. J. 2010. Galaxy formation theory. *Physics Reports*, **495**(Oct.), 33–86.

Benson, A. J., Frenk, C. S., Baugh, C. M., Cole, S., and Lacey, C. G. 2003. The effects of photoionization on galaxy formation - III. Environmental dependence in the luminosity function. *MNRAS*, **343**(Aug.), 679–691.

Besla, G., Kallivayalil, N., Hernquist, L., van der Marel, R. P., Cox, T. J., and Kereš, D. 2012. The role of dwarf galaxy interactions in shaping the Magellanic System and implications for Magellanic Irregulars. *MNRAS*, **421**(Apr.), 2109–2138.

Bird, S., Vogelsberger, M., Haehnelt, M., Sijacki, D., Genel, S., Torrey, P., Springel, V., and Hernquist, L. 2014. Damped Lyman α absorbers as a probe of stellar feedback. *MNRAS*, **445**(Dec.), 2313–2324.

Bird, S., Haehnelt, M., Neeleman, M., Genel, S., Vogelsberger, M., and Hernquist, L. 2015. Reproducing the kinematics of damped Lyman α systems. *MNRAS*, **447**(Feb.), 1834–1846.

Blumenthal, G. R., Faber, S. M., Primack, J. R., and Rees, M. J. 1984. Formation of galaxies and large-scale structure with cold dark matter. *Nature*, **311**(Oct.), 517–525.

Blumenthal, G. R., Faber, S. M., Flores, R., and Primack, J. R. 1986. Contraction of dark matter galactic halos due to baryonic infall. *ApJ*, **301**(Feb.), 27–34.

Boylan-Kolchin, M., Springel, V., White, S. D. M., Jenkins, A., and Lemson, G. 2009. Resolving cosmic structure formation with the Millennium-II Simulation. *MNRAS*, **398**(Sept.), 1150–1164.

Boylan-Kolchin, M., Bullock, J. S., and Kaplinghat, M. 2011. Too big to fail? The puzzling darkness of massive Milky Way subhaloes. *MNRAS*, **415**(July), L40–L44.

Boylan-Kolchin, M., Bullock, J. S., and Kaplinghat, M. 2012. The Milky Way's bright satellites as an apparent failure of ΛCDM. *MNRAS*, **422**(May), 1203–1218.

Breddels, M. A., and Helmi, A. 2013. Model comparison of the dark matter profiles of Fornax, Sculptor, Carina and Sextans. *Astronomy & Astrophysics*, **558**(Oct.), A35.

Breddels, M. A., and Helmi, A. 2014. Complexity on Dwarf Galaxy Scales: A Bimodal Distribution Function in Sculptor. *ApJL*, **791**(Aug.), L3.

Brennan, R., Pandya, V., Somerville, R. S., Barro, G., Taylor, E. N., Wuyts, S., Bell, E. F., Dekel, A., Ferguson, H. C., McIntosh, D. H., Papovich, C., and Primack, J. 2015. Quenching and Morphological Transformation in Semi-Analytic Models and CANDELS. *ArXiv e-prints*, Jan.

Brooks, A. 2014. Re-examining astrophysical constraints on the dark matter model. *Annalen der Physik*, **526**(Aug.), 294–308.

Brooks, A. M., and Zolotov, A. 2014. Why Baryons Matter: The Kinematics of Dwarf Spheroidal Satellites. *ApJ*, **786**(May), 87.

Bullock, J. S., Kravtsov, A. V., and Weinberg, D. H. 2000. Reionization and the Abundance of Galactic Satellites. *ApJ*, **539**(Aug.), 517–521.

Bullock, J. S., Kolatt, T. S., Sigad, Y., Somerville, R. S., Kravtsov, A. V., Klypin, A. A., Primack, J. R., and Dekel, A. 2001. Profiles of dark haloes: evolution, scatter and environment. *MNRAS*, **321**(Mar.), 559–575.

Bullock, J. S., Stewart, K. R., Kaplinghat, M., Tollerud, E. J., and Wolf, J. 2010. Stealth Galaxies in the Halo of the Milky Way. *ApJ*, **717**(July), 1043–1053.

Busha, M. T., Wechsler, R. H., Behroozi, P. S., Gerke, B. F., Klypin, A. A., and Primack, J. R. 2011a. Statistics of Satellite Galaxies around Milky-Way-like Hosts. *ApJ*, **743**(Dec.), 117.

Busha, M. T., Marshall, P. J., Wechsler, R. H., Klypin, A., and Primack, J. 2011b. The Mass Distribution and Assembly of the Milky Way from the Properties of the Magellanic Clouds. *ApJ*, **743**(Dec.), 40.

Carlberg, R. G. 2012. Dark Matter Sub-halo Counts via Star Stream Crossings. *ApJ*, **748**(Mar.), 20.

Carlberg, R. G., and Grillmair, C. J. 2013. Gaps in the GD-1 Star Stream. *ApJ*, **768**(May), 171.

Carlberg, R. G., Grillmair, C. J., and Hetherington, N. 2012. The Pal 5 Star Stream Gaps. *ApJ*, **760**(Nov.), 75.

Ceverino, D., and Klypin, A. 2009. The Role of Stellar Feedback in the Formation of Galaxies. *ApJ*, **695**(Apr.), 292–309.

Ceverino, D., Dekel, A., Mandelker, N., Bournaud, F., Burkert, A., Genzel, R., and Primack, J. 2012. Rotational support of giant clumps in high-z disc galaxies. *MNRAS*, **420**(Mar.), 3490–3520.

Ceverino, D., Klypin, A., Klimek, E. S., Trujillo-Gomez, S., Churchill, C. W., Primack, J., and Dekel, A. 2014. Radiative feedback and the low efficiency of galaxy formation in low-mass haloes at high redshift. *MNRAS*, **442**(Aug.), 1545–1559.

Ceverino, D., Dekel, A., Tweed, D., and Primack, J. 2015a. Early formation of massive, compact, spheroidal galaxies with classical profiles by violent disc instability or mergers. *MNRAS*, **447**(Mar.), 3291–3310.

Ceverino, D., Primack, J., and Dekel, A. 2015b. Formation of elongated galaxies with low masses at high redshift. *ArXiv e-prints*, Apr.

Chen, J., Koushiappas, S. M., and Zentner, A. R. 2011. The Effects of Halo-to-halo Variation on Substructure Lensing. *ApJ*, **741**(Nov.), 117.

Conroy, C., Wechsler, R. H., and Kravtsov, A. V. 2006. Modeling Luminosity-dependent Galaxy Clustering through Cosmic Time. *ApJ*, **647**(Aug.), 201–214.

Cowie, L. L., Songaila, A., Hu, E. M., and Cohen, J. G. 1996. New Insight on Galaxy Formation and Evolution From Keck Spectroscopy of the Hawaii Deep Fields. *AJ*, **112**(Sept.), 839.

Dalal, N., and Kochanek, C. S. 2002. Direct Detection of Cold Dark Matter Substructure. *ApJ*, **572**(June), 25–33.

Danovich, M., Dekel, A., Hahn, O., Ceverino, D., and Primack, J. 2015. Four phases of angular-momentum buildup in high-z galaxies: from cosmic-web streams through an extended ring to disc and bulge. *MNRAS*, **449**(May), 2087–2111.

Dekel, A., and Silk, J. 1986. The origin of dwarf galaxies, cold dark matter, and biased galaxy formation. *ApJ*, **303**(Apr.), 39–55.

Dekel, A., and Woo, J. 2003. Feedback and the fundamental line of low-luminosity low-surface-brightness/dwarf galaxies. *MNRAS*, **344**(Oct.), 1131–1144.

Diemand, J., Kuhlen, M., and Madau, P. 2007. Formation and Evolution of Galaxy Dark Matter Halos and Their Substructure. *ApJ*, **667**(Oct.), 859–877.

Diemand, J., Kuhlen, M., Madau, P., Zemp, M., Moore, B., Potter, D., and Stadel, J. 2008. Clumps and streams in the local dark matter distribution. *Nature*, **454**(Aug.), 735–738.

Elbert, O. D., Bullock, J. S., Garrison-Kimmel, S., Rocha, M., Oñorbe, J., and Peter, A. H. G. 2014. Core Formation in Dwarf Halos with Self Interacting Dark Matter: No Fine-Tuning Necessary. *ArXiv e-prints*, Dec.

Faucher-Giguère, C.-A., Hopkins, P. F., Kereš, D., Muratov, A. L., Quataert, E., and Murray, N. 2015. Neutral hydrogen in galaxy haloes at the peak of the cosmic star formation history. *MNRAS*, **449**(May), 987–1003.

Feldmann, R., and Spolyar, D. 2015. Detecting dark matter substructures around the Milky Way with Gaia. *MNRAS*, **446**(Jan.), 1000–1012.

Flores, R. A., and Primack, J. R. 1994. Observational and theoretical constraints on singular dark matter halos. *ApJL*, **427**(May), L1–L4.

Fukugita, M., and Peebles, P. J. E. 2004. The Cosmic Energy Inventory. *ApJ*, **616**(Dec.), 643–668.

Gnedin, O. Y., Ceverino, D., Gnedin, N. Y., Klypin, A. A., Kravtsov, A. V., Levine, R., Nagai, D., and Yepes, G. 2011. Halo Contraction Effect in Hydrodynamic Simulations of Galaxy Formation. *ArXiv e-prints*, Aug.

Governato, F., Brook, C., Mayer, L., Brooks, A., Rhee, G., Wadsley, J., Jonsson, P., Willman, B., Stinson, G., Quinn, T., and Madau, P. 2010. Bulgeless dwarf galaxies and dark matter cores from supernova-driven outflows. *Nature*, **463**(Jan.), 203–206.

Governato, F., Zolotov, A., Pontzen, A., Christensen, C., Oh, S. H., Brooks, A. M., Quinn, T., Shen, S., and Wadsley, J. 2012. Cuspy no more: how outflows affect the central dark matter and baryon distribution in Λ cold dark matter galaxies. *MNRAS*, **422**(May), 1231–1240.

Governato, F., Weisz, D., Pontzen, A., Loebman, S., Reed, D., Brooks, A. M., Behroozi, P., Christensen, C., Madau, P., Mayer, L., Shen, S., Walker, M., Quinn, T., Keller, B. W., and Wadsley, J. 2015. Faint dwarfs as a test of DM models: WDM versus CDM. *MNRAS*, **448**(Mar.), 792–803.

Guedes, J., Callegari, S., Madau, P., and Mayer, L. 2011. Forming Realistic Late-type Spirals in a ΛCDM Universe: The Eris Simulation. *ApJ*, **742**(Dec.), 76.

Guo, Y., Giavalisco, M., Ferguson, H. C., Cassata, P., and Koekemoer, A. M. 2012. Multi-wavelength View of Kiloparsec-scale Clumps in Star-forming Galaxies at z ˜ 2. *ApJ*, **757**(Oct.), 120.

Guo, Y., Ferguson, H. C., Bell, E. F., Koo, D. C., Conselice, C. J., Giavalisco, M., Kassin, S., Lu, Y., Lucas, R., Mandelker, N., McIntosh, D. M., Primack, J. R., Ravindranath, S., Barro, G., Ceverino, D., Dekel, A., Faber, S. M., Fang, J. J., Koekemoer, A. M., Noeske, K., Rafelski, M., and Straughn, A. 2015. Clumpy Galaxies in CANDELS. I. The Definition of UV Clumps and the Fraction of Clumpy Galaxies at 0.5 ¡ z ¡ 3. *ApJ*, **800**(Feb.), 39.

Harvey, D., Massey, R., Kitching, T., Taylor, A., and Tittley, E. 2015. The non-gravitational interactions of dark matter in colliding galaxy clusters. *Science*, **347**(Mar.), 1462–1465.

Hayward, C. C., Kereš, D., Jonsson, P., Narayanan, D., Cox, T. J., and Hernquist, L. 2011. What Does a Submillimeter Galaxy Selection Actually Select? The Dependence of Submillimeter Flux Density on Star Formation Rate and Dust Mass. *ApJ*, **743**(Dec.), 159.

Hayward, C. C., Behroozi, P. S., Somerville, R. S., Primack, J. R., Moreno, J., and Wechsler, R. H. 2013. Spatially unassociated galaxies contribute significantly to the blended submillimetre galaxy population: predictions for follow-up observations of ALMA sources. *MNRAS*, **434**(Sept.), 2572–2581.

Hearin, A. P., and Watson, D. F. 2013. The dark side of galaxy colour. *MNRAS*, **435**(Oct.), 1313–1324.

Hearin, A. P., Watson, D. F., Becker, M. R., Reyes, R., Berlind, A. A., and Zentner, A. R. 2014. The dark side of galaxy colour: evidence from new SDSS measurements of galaxy clustering and lensing. *MNRAS*, **444**(Oct.), 729–743.

Hezaveh, Y., Dalal, N., Holder, G., Kuhlen, M., Marrone, D., Murray, N., and Vieira, J. 2013. Dark Matter Substructure Detection Using Spatially Resolved Spectroscopy of Lensed Dusty Galaxies. *ApJ*, **767**(Apr.), 9.

Hezaveh, Y., Dalal, N., Holder, G., Kisner, T., Kuhlen, M., and Perreault Levasseur, L. 2014. Measuring the power spectrum of dark matter substructure using strong gravitational lensing. *ArXiv e-prints*, Mar.

Hlozek, R., Dunkley, J., Addison, G., Appel, J. W., Bond, J. R., Sofia Carvalho, C., Das, S., Devlin, M. J., Dünner, R., Essinger-Hileman, T., Fowler, J. W., Gallardo, P., Hajian, A., Halpern, M., Hasselfield, M., Hilton, M., Hincks, A. D., Hughes, J. P., Irwin, K. D., Klein, J., Kosowsky, A., Marriage, T. A., Marsden, D., Menanteau, F., Moodley, K., Niemack, M. D., Nolta, M. R., Page, L. A., Parker, L., Partridge, B., Rojas, F., Sehgal, N., Sherwin, B., Sievers, J., Spergel, D. N., Staggs, S. T., Swetz, D. S., Switzer, E. R., Thornton, R., and Wollack, E. 2012. The Atacama Cosmology Telescope: A Measurement of the Primordial Power Spectrum. *ApJ*, **749**(Apr.), 90.

Hopkins, P. F. 2014. GIZMO: A New Class of Accurate, Mesh-Free Hydrodynamic Simulation Methods. *ArXiv e-prints*, Sept.

Hopkins, P. F., Quataert, E., and Murray, N. 2012. Stellar feedback in galaxies and the origin of galaxy-scale winds. *MNRAS*, **421**(Apr.), 3522–3537.

Hopkins, P. F., Kereš, D., Oñorbe, J., Faucher-Giguère, C.-A., Quataert, E., Murray, N., and Bullock, J. S. 2014. Galaxies on FIRE (Feedback In Realistic Environments): stellar feedback explains cosmologically inefficient star formation. *MNRAS*, **445**(Nov.), 581–603.

Horiuchi, S., Humphrey, P. J., Oñorbe, J., Abazajian, K. N., Kaplinghat, M., and Garrison-Kimmel, S. 2014. Sterile neutrino dark matter bounds from galaxies of the Local Group. *Phys. Rev. D*, **89**(2), 025017.

Jardel, J. R., and Gebhardt, K. 2012. The Dark Matter Density Profile of the Fornax Dwarf. *ApJ*, **746**(Feb.), 89.

Jardel, J. R., and Gebhardt, K. 2013. Variations in a Universal Dark Matter Profile for Dwarf Spheroidals. *ApJL*, **775**(Sept.), L30.

Jonsson, P. 2006. SUNRISE: polychromatic dust radiative transfer in arbitrary geometries. *MNRAS*, **372**(Oct.), 2–20.

Jonsson, P., and Primack, J. R. 2010. Accelerating dust temperature calculations with graphics-processing units. *Nature*, **15**(Aug.), 509–514.

Jonsson, P., Cox, T. J., Primack, J. R., and Somerville, R. S. 2006. Simulations of Dust in Interacting Galaxies. I. Dust Attenuation. *ApJ*, **637**(Jan.), 255–268.

Jonsson, P., Groves, B. A., and Cox, T. J. 2010. High-resolution panchromatic spectral models of galaxies including photoionization and dust. *MNRAS*, **403**(Mar.), 17–44.

Keeton, C. R., and Moustakas, L. A. 2009. A New Channel for Detecting Dark Matter Substructure in Galaxies: Gravitational Lens Time Delays. *ApJ*, **699**(July), 1720–1731.

Kim, J.-h., Abel, T., Agertz, O., Bryan, G. L., Ceverino, D., Christensen, C., Conroy, C., Dekel, A., Gnedin, N. Y., Goldbaum, N. J., Guedes, J., Hahn, O., Hobbs, A., Hopkins, P. F., Hummels, C. B., Iannuzzi, F., Keres, D., Klypin, A., Kravtsov, A. V., Krumholz, M. R., Kuhlen, M., Leitner, S. N., Madau, P., Mayer, L., Moody, C. E., Nagamine, K., Norman, M. L., Onorbe, J., O'Shea, B. W., Pillepich, A., Primack, J. R., Quinn, T., Read, J. I., Robertson, B. E., Rocha, M., Rudd, D. H., Shen, S., Smith, B. D., Szalay, A. S., Teyssier, R., Thompson, R., Todoroki, K., Turk, M. J., Wadsley, J. W., Wise, J. H., Zolotov, A., and AGORA Collaboration29, t. 2014. The AGORA High-resolution Galaxy Simulations Comparison Project. *ApJS*, **210**(Jan.), 14.

Kirby, E. N., Martin, C. L., and Finlator, K. 2011. Metals Removed by Outflows from Milky Way Dwarf Spheroidal Galaxies. *ApJL*, **742**(Dec.), L25.

Klypin, A., Kravtsov, A. V., Valenzuela, O., and Prada, F. 1999. Where Are the Missing Galactic Satellites? *ApJ*, **522**(Sept.), 82–92.

Klypin, A., Karachentsev, I., Makarov, D., and Nasonova, O. 2014a. Abundance of Field Galaxies. *ArXiv e-prints*, May.

Klypin, A., Yepes, G., Gottlober, S., Prada, F., and Hess, S. 2014b. MultiDark simulations: the story of dark matter halo concentrations and density profiles. *ArXiv e-prints*, Nov.

Klypin, A. A., Trujillo-Gomez, S., and Primack, J. 2011. Dark Matter Halos in the Standard Cosmological Model: Results from the Bolshoi Simulation. *ApJ*, **740**(Oct.), 102.

Kormendy, J., and Fisher, D. B. 2008 (Oct.). Secular Evolution in Disk Galaxies: Pseudobulge Growth and the Formation of Spheroidal Galaxies. Page 297 of: J. G. Funes & E. M. Corsini (ed), *Formation and Evolution of Galaxy Disks*. Astronomical Society of the Pacific Conference Series, vol. 396.

Kravtsov, A. 2010. Dark Matter Substructure and Dwarf Galactic Satellites. *Advances in Astronomy*, **2010**.

Kravtsov, A. V., Klypin, A. A., and Khokhlov, A. M. 1997. Adaptive Refinement Tree: A New High-Resolution N-Body Code for Cosmological Simulations. *ApJS*, **111**(July), 73–+.

Kravtsov, A. V., Berlind, A. A., Wechsler, R. H., Klypin, A. A., Gottlöber, S., Allgood, B., and Primack, J. R. 2004. The Dark Side of the Halo Occupation Distribution. *ApJ*, **609**(July), 35–49.

Kuhlen, M., Vogelsberger, M., and Angulo, R. 2012. Numerical simulations of the dark universe: State of the art and the next decade. *Physics of the Dark Universe*, **1**(Nov.), 50–93.

Kuzio de Naray, R., and Spekkens, K. 2011. Do Baryons Alter the Halos of Low Surface Brightness Galaxies? *ApJL*, **741**(Nov.), L29.

Kuzio de Naray, R., Martinez, G. D., Bullock, J. S., and Kaplinghat, M. 2010. The Case Against Warm or Self-Interacting Dark Matter as Explanations for Cores in Low Surface Brightness Galaxies. *ApJL*, **710**(Feb.), L161–L166.

Lagos, C. d. P., Crain, R. A., Schaye, J., Furlong, M., Frenk, C. S., Bower, R. G., Schaller, M., Theuns, T., Trayford, J. W., Bahe, Y. M., and Dalla Vecchia, C. 2015. Molecular hydrogen abundances of galaxies in the EAGLE simulations. *ArXiv e-prints*, Mar.

Lahav, O., Lilje, P. B., Primack, J. R., and Rees, M. J. 1991. Dynamical effects of the cosmological constant. *MNRAS*, **251**(July), 128–136.

Liu, L., Gerke, B. F., Wechsler, R. H., Behroozi, P. S., and Busha, M. T. 2011. How Common are the Magellanic Clouds? *ApJ*, **733**(May), 62.

Lovell, M. R., Eke, V., Frenk, C. S., Gao, L., Jenkins, A., Theuns, T., Wang, J., White, S. D. M., Boyarsky, A., and Ruchayskiy, O. 2012. The haloes of bright satellite galaxies in a warm dark matter universe. *MNRAS*, **420**(Mar.), 2318–2324.

Ma, X., Hopkins, P. F., Faucher-Giguere, C.-A., Zolman, N., Muratov, A. L., Keres, D., and Quataert, E. 2015. The Origin and Evolution of the Galaxy Mass-Metallicity Relation. *ArXiv e-prints*, Apr.

Macciò, A. V., Dutton, A. A., van den Bosch, F. C., Moore, B., Potter, D., and Stadel, J. 2007. Concentration, spin and shape of dark matter haloes: scatter and the dependence on mass and environment. *MNRAS*, **378**(June), 55–71.

Macciò, A. V., Paduroiu, S., Anderhalden, D., Schneider, A., and Moore, B. 2012a. Cores in warm dark matter haloes: a Catch 22 problem. *MNRAS*, **424**(Aug.), 1105–1112.

Macciò, A. V., Stinson, G., Brook, C. B., Wadsley, J., Couchman, H. M. P., Shen, S., Gibson, B. K., and Quinn, T. 2012b. Halo Expansion in Cosmological Hydro Simulations: Toward a Baryonic Solution of the Cusp/Core Problem in Massive Spirals. *ApJL*, **744**(Jan.), L9.

Macciò, A. V., Paduroiu, S., Anderhalden, D., Schneider, A., and Moore, B. 2013. Erratum: Cores in warm dark matter haloes: a Catch 22 problem. *MNRAS*, **428**(Feb.), 3715–3716.

Madau, P., Shen, S., and Governato, F. 2014. Dark Matter Heating and Early Core Formation in Dwarf Galaxies. *ApJL*, **789**(July), L17.

Maller, A. H., and Dekel, A. 2002. Towards a resolution of the galactic spin crisis: mergers, feedback and spin segregation. *MNRAS*, **335**(Sept.), 487–498.

Mandelker, N., Dekel, A., Ceverino, D., Tweed, D., Moody, C. E., and Primack, J. 2014. The population of giant clumps in simulated high-z galaxies: in situ and ex situ migration and survival. *MNRAS*, **443**(Oct.), 3675–3702.

Massey, R., Williams, L., Smit, R., Swinbank, M., Kitching, T. D., Harvey, D., Jauzac, M., Israel, H., Clowe, D., Edge, A., Hilton, M., Jullo, E., Leonard, A., Liesenborgs, J., Merten, J., Mohammed, I., Nagai, D., Richard, J., Robertson, A., Saha, P., Santana, R., Stott, J., and Tittley, E. 2015. The behaviour of dark matter associated with four bright cluster galaxies in the 10 kpc core of Abell 3827. *MNRAS*, **449**(June), 3393–3406.

Metcalf, R. B., and Amara, A. 2012. Small-scale structures of dark matter and flux anomalies in quasar gravitational lenses. *MNRAS*, **419**(Feb.), 3414–3425.

Metcalf, R. B., and Madau, P. 2001. Compound Gravitational Lensing as a Probe of Dark Matter Substructure within Galaxy Halos. *ApJ*, **563**(Dec.), 9–20.

Metcalf, R. B., and Silk, J. 2007. New Constraints on Macroscopic Compact Objects as Dark Matter Candidates from Gravitational Lensing of Type Ia Supernovae. *Physical Review Letters*, **98**(7), 071302.

Metcalf, R. B., and Zhao, H. 2002. Flux Ratios as a Probe of Dark Substructures in Quadruple-Image Gravitational Lenses. *ApJL*, **567**(Mar.), L5–L8.

Moody, C. E., Guo, Y., Mandelker, N., Ceverino, D., Mozena, M., Koo, D. C., Dekel, A., and Primack, J. 2014. Star formation and clumps in cosmological galaxy simulations with radiation pressure feedback. *MNRAS*, **444**(Oct.), 1389–1399.

Moore, B. 1994. Evidence against dissipation-less dark matter from observations of galaxy haloes. *Nature*, **370**(Aug.), 629–631.

Moore, B., Ghigna, S., Governato, F., Lake, G., Quinn, T., Stadel, J., and Tozzi, P. 1999. Dark Matter Substructure within Galactic Halos. *ApJL*, **524**(Oct.), L19–L22.

Moustakas, L. A., and Metcalf, R. B. 2003. Detecting dark matter substructure spectroscopically in strong gravitational lenses. *MNRAS*, **339**(Mar.), 607–615.

Navarro, J. F., and Steinmetz, M. 2000. The Core Density of Dark Matter Halos: A Critical Challenge to the ΛCDM Paradigm? *ApJ*, **528**(Jan.), 607–611.

Navarro, J. F., Frenk, C. S., and White, S. D. M. 1996. The Structure of Cold Dark Matter Halos. *ApJ*, **462**(May), 563.

Ngan, W. H. W., and Carlberg, R. G. 2014. Using Gaps in N-body Tidal Streams to Probe Missing Satellites. *ApJ*, **788**(June), 181.

Nierenberg, A. M., Treu, T., Wright, S. A., Fassnacht, C. D., and Auger, M. W. 2014. Detection of substructure with adaptive optics integral field spectroscopy of the gravitational lens B1422+231. *MNRAS*, **442**(Aug.), 2434–2445.

Nipoti, C., and Binney, J. 2015. Early flattening of dark matter cusps in dwarf spheroidal galaxies. *MNRAS*, **446**(Jan.), 1820–1828.

Oñorbe, J., Boylan-Kolchin, M., Bullock, J. S., Hopkins, P. F., Kerěs, D., Faucher-Giguère, C.-A., Quataert, E., and Murray, N. 2015. Forged in FIRE: cusps, cores, and baryons in low-mass dwarf galaxies. *ArXiv e-prints*, Feb.

Oman, K. A., Navarro, J. F., Fattahi, A., Frenk, C. S., Sawala, T., White, S. D. M., Bower, R., Crain, R. A., Furlong, M., Schaller, M., Schaye, J., and Theuns, T. 2015. The unexpected diversity of dwarf galaxy rotation curves. *ArXiv e-prints*, Apr.

Papastergis, E., Martin, A. M., Giovanelli, R., and Haynes, M. P. 2011. The Velocity Width Function of Galaxies from the 40% ALFALFA Survey: Shedding Light on the Cold Dark Matter Overabundance Problem. *ApJ*, **739**(Sept.), 38.

Planck Collaboration, Ade, P. A. R., Aghanim, N., Arnaud, M., Ashdown, M., Aumont, J., Baccigalupi, C., Banday, A. J., Barreiro, R. B., Bartlett, J. G., and et al. 2015a. Planck 2015 results. XIII. Cosmological parameters. *ArXiv e-prints*, Feb.

Planck Collaboration, Ade, P. A. R., Aghanim, N., Arnaud, M., Arroja, F., Ashdown, M., Aumont, J., Baccigalupi, C., Ballardini, M., Banday, A. J., and et al. 2015b. Planck 2015 results. XVII. Constraints on primordial non-Gaussianity. *ArXiv e-prints*, Feb.

Polisensky, E., and Ricotti, M. 2011. Constraints on the dark matter particle mass from the number of Milky Way satellites. *Phys. Rev. D*, **83**(4), 043506.

Pontzen, A., and Governato, F. 2012. How supernova feedback turns dark matter cusps into cores. *MNRAS*, Mar., 2641.

Pooley, D., Rappaport, S., Blackburne, J. A., Schechter, P. L., and Wambsganss, J. 2012. X-Ray and Optical Flux Ratio Anomalies in Quadruply Lensed Quasars. II. Mapping the Dark Matter Content in Elliptical Galaxies. *ApJ*, **744**(Jan.), 111.

Porter, L. A., Somerville, R. S., Primack, J. R., Croton, D. J., Covington, M. D., Graves, G. J., and Faber, S. M. 2014a. Modelling the ages and metallicities of early-type galaxies in Fundamental Plane space. *MNRAS*, **445**(Dec.), 3092–3104.

Porter, L. A., Somerville, R. S., Primack, J. R., and Johansson, P. H. 2014b. Understanding the structural scaling relations of early-type galaxies. *MNRAS*, **444**(Oct.), 942–960.

Prada, F., Klypin, A. A., Cuesta, A. J., Betancort-Rijo, J. E., and Primack, J. 2012. Halo concentrations in the standard Λ cold dark matter cosmology. *MNRAS*, **423**(July), 3018–3030.

Primack, Joel R. 1984. Dark Matter, Galaxies and Large Scale Structure in the Universe. *Proc.Int.Sch.Phys.Fermi*, **92**, 140.

Primack, Joel R., and Abrams, Nancy Ellen. 2006. *The View from the Center of the Universe: Discovering Our Extraordinary Place in the Cosmos*. Riverhead.

Primack, Joel R., and Blumenthal, George R. 1984. Growth of Perturbations between Horizon Crossing and Matter Dominance: Implications for Galaxy Formation. *Astrophys.Space Sci.Libr.*, **111**, 435–440.

Rahmati, A., Schaye, J., Bower, R. G., Crain, R. A., Furlong, M., Schaller, M., and Theuns, T. 2015. The distribution of neutral hydrogen around high-redshift galaxies and quasars in the EAGLE simulation. *ArXiv e-prints*, Mar.

Reddick, R. M., Wechsler, R. H., Tinker, J. L., and Behroozi, P. S. 2013. The Connection between Galaxies and Dark Matter Structures in the Local Universe. *ApJ*, **771**(July), 30.

Reddick, R. M., Tinker, J. L., Wechsler, R. H., and Lu, Y. 2014. Cosmological Constraints from Galaxy Clustering and the Mass-to-number Ratio of Galaxy Clusters: Marginalizing over the Physics of Galaxy Formation. *ApJ*, **783**(Mar.), 118.

Richardson, T., and Fairbairn, M. 2014. On the dark matter profile in Sculptor: breaking the β degeneracy with Virial shape parameters. *MNRAS*, **441**(June), 1584–1600.

Riebe, K., Partl, A. M., Enke, H., Forero-Romero, J., Gottlöber, S., Klypin, A., Lemson, G., Prada, F., Primack, J. R., Steinmetz, M., and Turchaninov, V. 2013. The MultiDark Database: Release of the Bolshoi and MultiDark cosmological simulations. *Astronomische Nachrichten*, **334**(Aug.), 691–708.

Sawala, T., Scannapieco, C., and White, S. 2012. Local Group dwarf galaxies: nature and nurture. *MNRAS*, **420**(Feb.), 1714–1730.

Sawala, T., Frenk, C. S., Fattahi, A., Navarro, J. F., Bower, R. G., Crain, R. A., Dalla Vecchia, C., Furlong, M., Helly, J. C., Jenkins, A., Oman, K. A., Schaller, M., Schaye, J., Theuns, T., Trayford, J., and White, S. D. M. 2014. Local Group galaxies emerge from the dark. *ArXiv e-prints*, Dec.

Schaye, J., Crain, R. A., Bower, R. G., Furlong, M., Schaller, M., Theuns, T., Dalla Vecchia, C., Frenk, C. S., McCarthy, I. G., Helly, J. C., Jenkins, A., Rosas-Guevara, Y. M., White, S. D. M., Baes, M., Booth, C. M., Camps, P., Navarro, J. F., Qu, Y., Rahmati, A., Sawala, T., Thomas, P. A., and Trayford, J. 2015. The EAGLE project: simulating the evolution and assembly of galaxies and their environments. *MNRAS*, **446**(Jan.), 521–554.

Skillman, S. W., Warren, M. S., Turk, M. J., Wechsler, R. H., Holz, D. E., and Sutter, P. M. 2014. Dark Sky Simulations: Early Data Release. *ArXiv e-prints*, July.

Snyder, G. F., Torrey, P., Lotz, J. M., Genel, S., McBride, C. K., Vogelsberger, M., Pillepich, A., Nelson, D., Sales, L. V., Sijacki, D., Hernquist, L., and Springel, V. 2015. Galaxy Morphology and Star Formation in the Illustris Simulation at z=0. *ArXiv e-prints*, Feb.

Somerville, R. S. 2002. Can Photoionization Squelching Resolve the Substructure Crisis? *ApJL*, **572**(June), L23–L26.

Somerville, R. S., and Davé, R. 2014. Physical Models of Galaxy Formation in a Cosmological Framework. *ArXiv e-prints*, Dec.

Somerville, R. S., Gilmore, R. C., Primack, J. R., and Domínguez, A. 2012. Galaxy properties from the ultraviolet to the far-infrared: Λ cold dark matter models confront observations. *MNRAS*, **423**(July), 1992–2015.

Spergel, D. N., and Steinhardt, P. J. 2000. Observational Evidence for Self-Interacting Cold Dark Matter. *Physical Review Letters*, **84**(Apr.), 3760–3763.

Springel, V., White, S. D. M., Jenkins, A., Frenk, C. S., Yoshida, N., Gao, L., Navarro, J., Thacker, R., Croton, D., Helly, J., Peacock, J. A., Cole, S., Thomas, P., Couchman, H., Evrard, A., Colberg, J., and Pearce, F. 2005. Simulations of the formation, evolution and clustering of galaxies and quasars. *Nature*, **435**(June), 629–636.

Springel, V., Wang, J., Vogelsberger, M., Ludlow, A., Jenkins, A., Helmi, A., Navarro, J. F., Frenk, C. S., and White, S. D. M. 2008. The Aquarius Project: the subhaloes of galactic haloes. *MNRAS*, **391**(Dec.), 1685–1711.

Strigari, L. E., and Wechsler, R. H. 2012. The Cosmic Abundance of Classical Milky Way Satellites. *ApJ*, **749**(Apr.), 75.

Strigari, L. E., Barnabè, M., Marshall, P. J., and Blandford, R. D. 2012. Nomads of the Galaxy. *MNRAS*, **423**(June), 1856–1865.

Tasitsiomi, A., Kravtsov, A. V., Wechsler, R. H., and Primack, J. R. 2004. Modeling Galaxy-Mass Correlations in Dissipationless Simulations. *ApJ*, **614**(Oct.), 533–546.

Teyssier, R., Pontzen, A., Dubois, Y., and Read, J. I. 2013. Cusp-core transformations in dwarf galaxies: observational predictions. *MNRAS*, **429**(Mar.), 3068–3078.

The DES Collaboration, Bechtol, K., Drlica-Wagner, A., Balbinot, E., Pieres, A., Simon, J. D., Yanny, B., Santiago, B., Wechsler, R. H., Frieman, J., Walker, A. R., Williams, P., Rozo, E., Rykoff, E. S., Queiroz, A., Luque, E., Benoit-Levy, A., Bernstein, R. A., Tucker, D., Sevilla, I., Gruendl, R. A., da Costa, L. N., Fausti Neto, A., Maia, M. A. G., Abbott, T., Allam, S., Armstrong, R., Bauer, A. H., Bernstein, G. M., Bertin, E., Brooks, D., Buckley-Geer, E., Burke, D. L., Carnero Rosell, A., Castander, F. J., D'Andrea, C. B., DePoy, D. L., Desai, S., Diehl, H. T., Eifler, T. F., Estrada, J., Evrard, A. E., Fernandez, E., Finley, D. A., Flaugher, B., Gaztanaga, E., Gerdes, D., Girardi, L., Gladders, M., Gruen, D., Gutierrez, G., Hao, J., Honscheid, K., Jain, B., James, D., Kent, S., Kron, R., Kuehn, K., Kuropatkin, N., Lahav, O., Li, T. S., Lin, H., Makler, M., March, M., Marshall, J., Martini, P., Merritt, K. W., Miller, C., Miquel, R., Mohr, J., Neilsen, E., Nichol, R., Nord, B., Ogando, R., Peoples, J., Petravick, D., Plazas, A. A., Romer, A. K., Roodman, A., Sako, M., Sanchez, E., Scarpine, V., Schubnell, M., Smith, R. C., Soares-Santos, M., Sobreira, F., Suchyta, E., Swanson, M. E. C., Tarle, G., Thaler, J., Thomas, D., Wester, W., and Zuntz, J. 2015. Eight New Milky Way Companions Discovered in First-Year Dark Energy Survey Data. *ArXiv e-prints*, Mar.

Tisserand, P., Le Guillou, L., Afonso, C., Albert, J. N., Andersen, J., Ansari, R., Aubourg, É., Bareyre, P., Beaulieu, J. P., Charlot, X., Coutures, C., Ferlet, R., Fouqué, P., Glicenstein, J. F., Goldman, B., Gould, A., Graff, D., Gros, M., Haissinski, J., Hamadache, C., de Kat, J., Lasserre, T., Lesquoy, É., Loup,

C., Magneville, C., Marquette, J. B., Maurice, É., Maury, A., Milsztajn, A.,
Moniez, M., Palanque-Delabrouille, N., Perdereau, O., Rahal, Y. R., Rich, J.,
Spiro, M., Vidal-Madjar, A., Vigroux, L., Zylberajch, S., and EROS-2 Col-
laboration. 2007. Limits on the Macho content of the Galactic Halo from
the EROS-2 Survey of the Magellanic Clouds. *Astronomy & Astrophysics*,
469(July), 387–404.

Tollerud, E. J., Boylan-Kolchin, M., Barton, E. J., Bullock, J. S., and Trinh, C. Q.
2011. Small-scale Structure in the Sloan Digital Sky Survey and ΛCDM:
Isolated ~L ∗ Galaxies with Bright Satellites. *ApJ*, **738**(Sept.), 102.

Trujillo-Gomez, S., Klypin, A., Primack, J., and Romanowsky, A. J. 2011. Galax-
ies in ΛCDM with Halo Abundance Matching: Luminosity-Velocity Relation,
Baryonic Mass-Velocity Relation, Velocity Function, and Clustering. *ApJ*,
742(Nov.), 16.

Trujillo-Gomez, S., Klypin, A., Colín, P., Ceverino, D., Arraki, K. S., and Primack,
J. 2015. Low-mass galaxy assembly in simulations: regulation of early star
formation by radiation from massive stars. *MNRAS*, **446**(Jan.), 1140–1162.

van der Wel, A., Chang, Y.-Y., Bell, E. F., Holden, B. P., Ferguson, H. C., Gi-
avalisco, M., Rix, H.-W., Skelton, R., Whitaker, K., Momcheva, I., Brammer,
G., Kassin, S. A., Martig, M., Dekel, A., Ceverino, D., Koo, D. C., Mozena,
M., van Dokkum, P. G., Franx, M., Faber, S. M., and Primack, J. 2014. Ge-
ometry of Star-forming Galaxies from SDSS, 3D-HST, and CANDELS. *ApJL*,
792(Sept.), L6.

Vegetti, S., Koopmans, L. V. E., Bolton, A., Treu, T., and Gavazzi, R. 2010.
Detection of a dark substructure through gravitational imaging. *MNRAS*,
408(Nov.), 1969–1981.

Vegetti, S., Lagattuta, D. J., McKean, J. P., Auger, M. W., Fassnacht, C. D., and
Koopmans, L. V. E. 2012. Gravitational detection of a low-mass dark satellite
galaxy at cosmological distance. *Nature*, **481**(Jan.), 341–343.

Vegetti, S., Koopmans, L. V. E., Auger, M. W., Treu, T., and Bolton, A. S. 2014.
Inference of the cold dark matter substructure mass function at z = 0.2 using
strong gravitational lenses. *MNRAS*, **442**(Aug.), 2017–2035.

Viel, M., Becker, G. D., Bolton, J. S., and Haehnelt, M. G. 2013. Warm dark
matter as a solution to the small scale crisis: New constraints from high redshift
Lyman-α forest data. *Phys. Rev. D*, **88**(4), 043502.

Vogelsberger, M., Zavala, J., and Loeb, A. 2012. Subhaloes in self-interacting galac-
tic dark matter haloes. *MNRAS*, **423**(July), 3740–3752.

Vogelsberger, M., Genel, S., Springel, V., Torrey, P., Sijacki, D., Xu, D., Snyder,
G., Nelson, D., and Hernquist, L. 2014a. Introducing the Illustris Project:
simulating the coevolution of dark and visible matter in the Universe. *MNRAS*,
444(Oct.), 1518–1547.

Vogelsberger, M., Genel, S., Springel, V., Torrey, P., Sijacki, D., Xu, D., Snyder,
G., Bird, S., Nelson, D., and Hernquist, L. 2014b. Properties of galaxies re-
produced by a hydrodynamic simulation. *Nature*, **509**(May), 177–182.

Wadepuhl, M., and Springel, V. 2011. Satellite galaxies in hydrodynamical simula-
tions of Milky Way sized galaxies. *MNRAS*, **410**(Jan.), 1975–1992.

Walker, M. G., and Peñarrubia, J. 2011. A Method for Measuring (Slopes of) the
Mass Profiles of Dwarf Spheroidal Galaxies. *ApJ*, **742**(Nov.), 20.

Watson, D. F., Berlind, A. A., and Zentner, A. R. 2011. A Cosmic Coincidence:
The Power-law Galaxy Correlation Function. *ApJ*, **738**(Sept.), 22.

Wellons, S., Torrey, P., Ma, C.-P., Rodriguez-Gomez, V., Vogelsberger, M., Kriek, M., van Dokkum, P., Nelson, E., Genel, S., Pillepich, A., Springel, V., Sijacki, D., Snyder, G., Nelson, D., Sales, L., and Hernquist, L. 2015. The formation of massive, compact galaxies at z = 2 in the Illustris simulation. *MNRAS*, **449**(May), 361–372.

Woo, J., Courteau, S., and Dekel, A. 2008. Scaling relations and the fundamental line of the local group dwarf galaxies. *MNRAS*, **390**(Nov.), 1453–1469.

Wuyts, S., Förster Schreiber, N. M., Nelson, E. J., van Dokkum, P. G., Brammer, G., Chang, Y.-Y., Faber, S. M., Ferguson, H. C., Franx, M., Fumagalli, M., Genzel, R., Grogin, N. A., Kocevski, D. D., Koekemoer, A. M., Lundgren, B., Lutz, D., McGrath, E. J., Momcheva, I., Rosario, D., Skelton, R. E., Tacconi, L. J., van der Wel, A., and Whitaker, K. E. 2013. A CANDELS-3D-HST synergy: Resolved Star Formation Patterns at 0.7<z<1.5. *ApJ*, **779**(Dec.), 135.

Xu, D., Sluse, D., Gao, L., Wang, J., Frenk, C., Mao, S., Schneider, P., and Springel, V. 2015. How well can cold dark matter substructures account for the observed radio flux-ratio anomalies. *MNRAS*, **447**(Mar.), 3189–3206.

Xu, D. D., Mao, S., Cooper, A. P., Gao, L., Frenk, C. S., Angulo, R. E., and Helly, J. 2012. On the effects of line-of-sight structures on lensing flux-ratio anomalies in a ΛCDM universe. *MNRAS*, Feb., 2426.

Yoon, J. H., Johnston, K. V., and Hogg, D. W. 2011. Clumpy Streams from Clumpy Halos: Detecting Missing Satellites with Cold Stellar Structures. *ApJ*, **731**(Apr.), 58.

Zentner, A. R., and Bullock, J. S. 2003. Halo Substructure and the Power Spectrum. *ApJ*, **598**(Nov.), 49–72.

Zolotov, A., Dekel, A., Mandelker, N., Tweed, D., Inoue, S., DeGraf, C., Ceverino, D., Primack, J., Barro, G., and Faber, S. M. 2014. Compaction and Quenching of High-z Galaxies in Cosmological Simulations: Blue and Red Nuggets. *ArXiv e-prints*, Dec.

Zwaan, M. A., Meyer, M. J., and Staveley-Smith, L. 2010. The velocity function of gas-rich galaxies. *MNRAS*, **403**(Apr.), 1969–1977.